International Journal of Innovative
Computing, Information and Control
Volume **22**, Number **1**, February **2026**

ICIC International ©2026 ISSN 1349-4198
pp. **47–64**

MULTI-OBJECTIVE DAY-AHEAD OPTIMIZATION SCHEDULING OF MASSIVE AIR CONDITIONING LOADS CONSIDERING USER CONTROL WILLINGNESS BASED ON THE MTCMO ALGORITHM

Ji Wang[1,2], Jianlin Tang[1,2], Fan Zhang[1,2], Dawei Ren[3] and Zhengxun Guo[3,*]

[1]CSG Electric Power Research Institute
No. 11, Kexiang Road, Huangpu District, Guangzhou 510663, P. R. China
{ wangji; tangjl2; zhangfan4 }@csg.cn

[2]Guangdong Provincial Key Laboratory of Intelligent Measurement and Advanced Metering of Power Grid
No. 11, Kexiang Road, Huangpu District, Guangzhou 510663, P. R. China

[3]Foshan Graduate School of Innovation
Northeastern University
No. 3, Erzhi Industrial Avenue, Haichuang Dazu Robot Intelligent Manufacturing Center
Shunde District, Foshan 528312, P. R. China
rendw@mails.neu.edu.cn; *Corresponding author: 2310276@stu.neu.edu.cn

Received April 2025; revised July 2025

Abstract. *This study aims to address the critical challenge of integrating massive air conditioning (AC) loads into demand response (DR) programs while balancing user comfort, economic efficiency, and carbon emissions. Given the intermittent nature of renewable energy and the high flexibility of AC systems, we propose a multi-objective day-ahead scheduling strategy that combines start-stop control with temperature control. The strategy integrates dynamic carbon emission factors (based on real-time power grid data) to reflect spatial-temporal variations in emissions that incorporates user willingness to adjust temperature settings (ranging from 0°C to 3°C increments) and employs clustering analysis to group similar AC units by their thermal parameters (R, C, N, P). This clustering approach reduces computational complexity by 97.58% while maintaining acceptable comfort levels (7.92% fluctuation). To optimize the trade-offs between three objectives – user comfort (temperature deviation), electricity cost and carbon emission cost – we formulate a multi-objective optimization model and solve it using the multi-tasking constrained multi-objective optimization (MTCMO) algorithm, which outperforms traditional methods in global optimality. Simulation results for a 2,000-unit AC cluster demonstrate that the proposed strategy achieves a 23.23% reduction in electricity costs and a 27.53% reduction in carbon costs compared to unclustered control, while maintaining indoor temperatures within ±1°C of user preferences across varying willingness levels. The dynamic carbon emission factor integration enhances the economic viability of DR by aligning load adjustments with low-carbon power generation periods. This research provides a scalable framework for optimizing large-scale AC systems in smart grids advancing both operational efficiency and sustainability.*

Keywords: Air conditioning load, Dynamic carbon emission factor, Multi-objective optimization, Adjustment diversity, Analytic hierarchy process

1. **Introduction.** With the increase in CO_2 emissions and global climate warming, the urgent need to transition from coal-based fossil fuels to renewable energy sources has become apparent in recent years. However, the intermittent and variable characteristics of renewable energy make it challenging to achieve electrical balance by solely regulating

DOI: 10.24507/ijicic.22.01.47

the supply side [1-4]. Demand response (DR) can match the energy supply on the supply side with energy demand on the user side in real time, maintaining electrical balance between the supply and demand sides [5]. Accurate prediction of user-side energy consumption is crucial for implementing DR. According to the latest China Building Energy Consumption Report (2023), the total energy consumption during the building operation phase reached 1.21 billion tons of standard coal in 2022, accounting for 21.3% of China's total building energy consumption [6]. Among this, air conditioning energy consumption constituted 60% of the building operation phase energy consumption [7]. Air conditioning loads are characterized by high energy consumption and significant reduction potential, making the multi-objective control of large-scale air conditioners a key factor in effective DR implementation. Air conditioning loads, with their large scale, strong controllability, and significant adjustment potential, can contribute to balancing electricity supply and demand by aggregating and regulating large numbers of dispersed air conditioners, which is important for improving summer grid load characteristics [8].

The core of air conditioning load management lies in selecting appropriate control strategies and optimizing scheduling mechanisms. While control strategies determine how loads are modulated, scheduling mechanisms define when and to what extent these strategies are applied. At the control strategy level, two primary approaches dominate: direct load control (DLC) and temperature-based control strategies [9]. Currently, DLC serves as the mainstream methodology, encompassing direct switch control, periodic intermittent operation, and other variants [10]. Direct switch control strategies mechanically manage the on/off status of air conditioning units to achieve rapid load adjustment. While straightforward, this approach often neglects intelligent temperature adjustments, compromising user comfort [11-13]. [14] introduced an innovative cluster control strategy based on temperature data, utilizing temperature setpoints as response signals for intelligent management of aggregated air conditioning loads. Subsequent studies developed hourly-level fine-scheduling models that correlate temperature differences with power consumption, thereby enhancing scheduling efficiency while preserving user comfort [15]. Scheduling optimization mechanisms for these strategies will be discussed in the subsequent section.

To address the limitations of existing control strategies, we first analyze some previous related works and the gaps of works: direct switch control [16,17] achieves simplicity but sacrifices user comfort resulting to absence of joint electricity-carbon cost optimization (Gap 1); temperature-based scheduling [18,19] improves comfort at the cost of high computational complexity that some scalability issues are in large-scale systems (Gap 2); integrated frameworks [20,21] lack dynamic carbon-emission coupling in optimization that solution selection mechanisms are suboptimal (Gap 3).

We develop an enhanced two-layered framework to bridge these gaps that

1) integrates real-time dynamic carbon factors with user willingness models, enabling holistic cost optimization beyond [16,17]'s single-objective focus;
2) implements refined K-means clustering (using thermal-inertia similarity metrics), achieving 97.58% faster computation than [18,19] while maintaining comfort;
3) solves via enhanced MTCMO (with adaptive operators) and selects compromise solutions via AHP, improving robustness over [20,21].

At the cluster level, K-means groups AC units by thermal parameters, reducing computational time by 97.58% versus [18,19]. At the individual level, a day-ahead multi-objective model minimizes comfort deviation, electricity costs, and carbon costs using dynamic emission factors. The enhanced MTCMO generates Pareto fronts, with analytic hierarchy process (AHP) selecting the optimal compromise.

This work advances prior research by

1) Joint carbon-electricity optimization strategy: Resolves Gap (1) by integrating switch control, temperature control, and dynamic carbon electricity factor into a unified framework, enabling simultaneous minimization of electricity costs and dynamic spatiotemporal carbon modeling: enables real-time DR optimization via power flow-based emission factors;
2) Scalable clustering architecture: Overcomes Gap (2) via thermal-inertia based K-means clustering, achieving 97.58% computation efficiency gain versus [18,19] while maintaining comfort constraints in large-scale systems;
3) Robust multi-objective decision mechanism: Solves Gap (3) through enhanced MTC-MO with adaptive operators for Pareto-front generation, coupled with AHP-based compromise solution selection, improving scheduling stability.

The paper is organized as follows: Section 2 describes the problem formulation and literature review, Section 3 presents the proposed two-layered optimization framework, Section 4 details the algorithm implementation and case studies, and Section 5 discusses the results and conclusions.

2. **Air Conditioning Load Model.**

2.1. **First-order ETP model for air-conditioned buildings.**

The first-order equivalent thermal parameter (ETP) model can significantly reduce computation time while maintaining accuracy making it highly suitable for large-scale simulations [22]. Therefore, this paper adopts the first-order ETP model to represent the indoor temperature variation process of buildings with air conditioning. Assuming that the air conditioner is in cooling mode, the thermal dynamics of the air-conditioned space can be described as follows:

$$T^{\text{in}}(t) = T^{\text{out}}(t) - \left(T^{\text{out}}(t) - T^{\text{in}}(t)\right) e^{-\frac{\triangle t}{RC}} - \left(1 - e^{-\frac{\triangle t}{RC}}\right) QR \tag{1}$$

where $T^{\text{in}}(t)$ and $T^{\text{out}}(t)$ represent the indoor and outdoor temperatures at time t, respectively; $\triangle t$ denotes the duration from time t to $t+1$; R is the equivalent thermal resistance of the building where the air conditioner is installed; C is the equivalent thermal capacitance of the building; and Q represents the cooling capacity of the air conditioner.

The cooling capacity of the air conditioner is related to the coefficient of performance and the cooling power of the air conditioner, and can be expressed as

$$Q = N \cdot P \tag{2}$$

where N and P represent the coefficient of performance and the power of the air conditioner, respectively.

In real-world applications, two factors affect the operation of air conditioners: the on/off state (off and on) and the temperature state (standby and active) [23]. When the indoor temperature falls below the preset minimum temperature $T_{\min}$, the air conditioner can remain in the on state but its temperature state shifts to standby meaning it does not cool; thus, the indoor temperature gradually increases [24]. Conversely, when the indoor temperature exceeds the preset maximum temperature $T_{\max}$, the air conditioner activates its cooling mode causing the indoor temperature to gradually decrease. The indoor temperature control curves under different control strategies are shown in Figure 1. Due to direct control of the air conditioning load, the indoor temperature variation curve in Figure 1(a) will adjust to the new pattern depicted in Figure 1(b).

Based on the current temperature and on/off state, the operational status of the air conditioning load at the beginning of the next time period can be determined as follows:

$$k(t+1) = \begin{cases} 0 & u(t+1) = 0 \text{ or } T^{\text{in}}(t) < T_{\min} \\ 1 & u(t) = 0 \text{ or } u(t+1) = 1 \text{ and } T^{\text{in}}(t) \geq T_{\max} \\ k(t) & u(t) = 1 \text{ and } u(t+1) = 1 \text{ and } T_{\min} \leq T^{\text{in}}(t) \leq T_{\max} \\ 1 & u(t) = 1 \text{ and } u(t+1) = 1 \text{ and } T^{\text{in}}(t) \geq T_{\max} \end{cases} \tag{3}$$

where $u(t)$ denotes the on/off state of the air conditioning load at time t; $u(t) = 0$ and $u(t) = 1$ represent the air conditioner's off and on states at time t; $k(t) = 0$ and $k(t) = 1$ indicate the standby and active cooling states of the air conditioner, respectively.

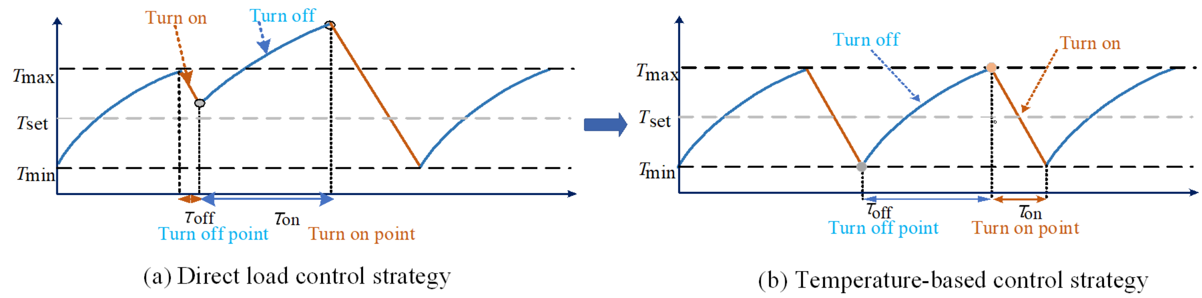

FIGURE 1. Temperature start-stop curve

2.2. **Operational characteristics of air conditioner switching.** Assuming that the air conditioner has reached a stable state before regulation, the indoor temperature T_t^{in} will remain at the maximum target temperature $T_{\max}$ before regulation. According to Equations (1) and (2), the time τ_{on} required for the indoor temperature to decrease from the maximum target temperature $T_{\max}$ to the minimum target temperature $T_{\min}$ can be expressed as

$$\tau_{\text{on}} = RC \ln \frac{T^{\text{out}}(t) - T_{\max} - RNP}{T^{\text{out}}(t) - T_{\min} - RNP} \tag{4}$$

When the air conditioner is turned off, the cooling power P is zero. Since the indoor temperature cannot exceed the upper temperature limit $T_{\max}$, the allowable shutdown duration of the air conditioner τ_{off} can be expressed as

$$\tau_{\text{off}} = RC \ln \frac{T^{\text{out}}(t) - T_{\max}}{T^{\text{out}}(t) - T_{\min}} \tag{5}$$

According to Equation (5), the allowable shutdown duration is dependent on the air conditioner's set temperature before regulation.

2.3. **Dynamic carbon emission factor.** The dynamic carbon emission factor is calculated based on real-time operational data from the power system to reflect the carbon emissions caused by electricity consumption at specific times and locations [28]. Its primary sources include

1) Real-time power dispatch data: This includes real-time generation data from power plants and fuel consumption data.
2) Electricity supply structure: The electricity supply structure from different generation units may vary over time, including the variable supply from renewable energy sources (e.g., wind and solar power).
3) Power flow in the grid: The dynamic changes in power flow within regional grids can also affect the carbon emission factor.
4) Grid carbon intensity data: This is based on the carbon intensity data of different types of power generation units.

Average carbon emission factors are typically based on annual or quarterly data and do not account for temporal fluctuations. In contrast, the dynamic carbon emission factor provides a more accurate reflection of instantaneous carbon emissions [25,26]. According to the principle of carbon emission flow transmission in the power grid, the schematic diagram is shown in Figure 2. Based on the proportional sharing principle, the average carbon emission intensity at each node is calculated considering both nodal inflows and external active power outputs. This intensity defines the carbon emission factor for both outgoing branch power and loads connected to the node [27].

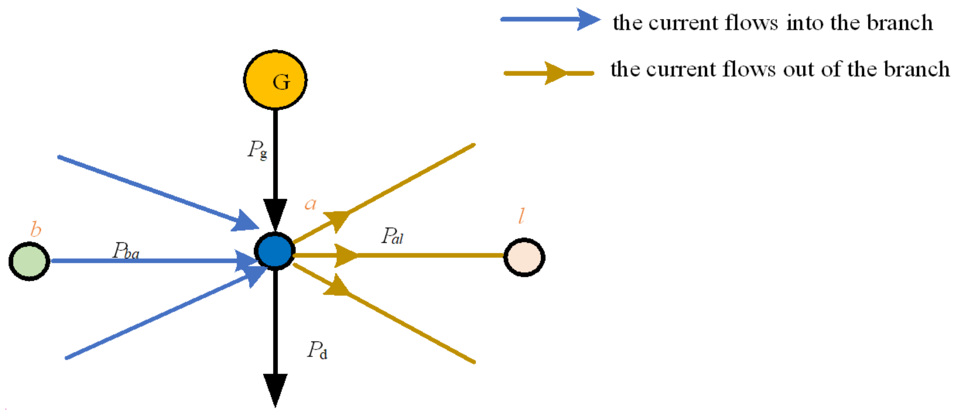

Figure 2. Grid carbon emission flow transmission schematic diagram

For a load node, the electricity carbon emission factor can be calculated using the following formula:

$$\delta_a = \frac{P_g \times \delta_g + \sum_{b \in \Omega_a} P_{ba} \times \delta_b}{P_g + \sum_{b \in \Omega_a} P_{ba}} \tag{6}$$

where δ_a ($kgCO_2/kWh$) and δ_b ($kgCO_2/kWh$) represent the electricity carbon emission factors for the load nodes; P_g (kW) represents the active power output of the generation unit connected to the load node a. δ_g ($kgCO_2/kWh$) is the average carbon emission factor of the generation unit connected to load node; P_{ba} (kW) represents the active power injected into the branch from load node b to load node a; Ω_a represents the set of nodes directly connected to load node a by branches.

3. Optimization Control Strategies for Air Conditioning Clusters.

Figure 3 simplifies framework for user electricity consumption behavior analysis and demand response modeling with a focus on air conditioning clusters. The simplified system framework is divided into three components: user electricity consumption behavior analysis, big-data-driven clustering analysis and demand response modeling [29]. The left section categorizes loads into industrial, commercial, residential, distribution, energy storage, charging infrastructure and other categories; with air conditioning clusters highlighted as a critical subset due to their significant impact on peak demand. The central module employs clustering techniques to segment users based on consumption behavior patterns and regulatory assessment utilizing data such as user electricity budgets and device-level energy consumption. The right section constructs an air conditioning response regulation model to establish dynamic targets and constraints, optimizing grid flexibility and carbon reduction benefits.

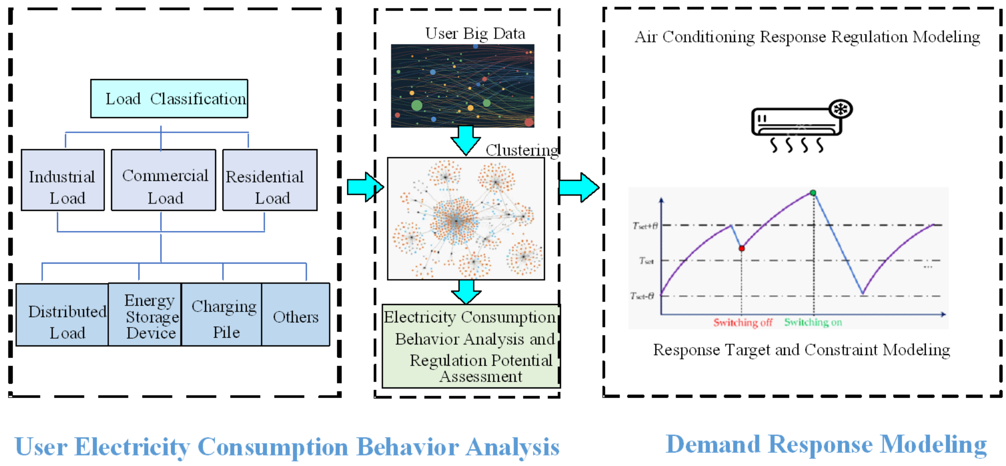

FIGURE 3. Block diagram of air conditioning cluster clustering

3.1. Optimization control objective function.

In existing research, there is a significant focus on the economic and user experience aspects of control processes, with less attention given to factors such as energy efficiency and carbon emissions. It is important to note that the regulation of air conditioning loads should ensure the stability of power supply and the safety of equipment while comprehensively considering user preferences, economic factors, energy efficiency, and carbon emissions. To enhance the economic benefits of control strategies while improving the overall quality of control, priority should be given to users with lower energy efficiency and higher carbon emissions. These users should actively participate in load reduction, thereby promoting the high-quality development of air conditioning load regulation. This paper aims to maximize user comfort while minimizing electricity costs and carbon emission costs. The multi-objective optimization model for day-ahead scheduling of air conditioning loads can be described as follows:

$$\begin{cases} \min f_1 = \sum_{z=1}^{Z} \sum_{s=1}^{S} \omega_z(t) \times \left| T_z^{\text{avg}}(t) - T_z^{\text{set}}(t) \right| \\ \min f_2 = \sum_{z=1}^{Z} \sum_{s=1}^{S} k_z(t) \times \tau_{\text{on}} \times P \times \psi_e(t) \\ \min f_3 = \sum_{z=1}^{Z} \sum_{s=1}^{S} k_z(t) \times \tau_{\text{on}} \times P \times \psi_c(t) \times \sigma_z(t) \end{cases} \tag{7}$$

where f_1 represents the temperature comfort deviation function; f_2 represents the electricity cost function; f_3 represents the carbon emission cost function; Z is the number of users; $\omega_z(t)$ represents the temperature preference weight for the z-th user at time t; $T_z^{\text{avg}}(t)$ (°C) and $T_z^{\text{set}}(t)$ (°C) are the average room temperature and the preset ideal room temperature of the z-th user at the t-th moment, respectively; $k_z(t)$ indicates the on/off state of the air conditioner: value 0 represents off and value 1 represents on; S (h) indicates the total hours in a day; $\sigma_z(t)$ ($kgCO_2$/kWh) is the electricity carbon emission factor of the z-th user at the t-th moment; $\psi_e(t)$ (CNY/kWh) and $\psi_c(t)$ (CNY/$kgCO_2$) are the electricity price and carbon price at the t-th moment, respectively.

3.2. Conditions for analyzing optimization control algorithms.

• **Principles of Analytic Hierarchy Process**

AHP is a structured multi-criteria decision-making tool that helps decision-makers evaluate multiple options and determine the best choice by breaking down complex decision problems into a hierarchy of related elements and quantifying the weights (relative importance) of these elements through pairwise comparisons. The process involves decomposing the problem into simpler decision components and then synthesizing these components into a multi-layered model based on their relationships. The fundamental approach of AHP is to first decompose the problem and then integrate the results, simplifying a complex decision into a series of simpler decisions.

- Goal Level (Top Level): Optimal balance of the three objective functions;
- Criteria Level (Intermediate Level): Comfort, carbon emission cost, electricity cost;
- Alternatives Level: Different control strategies.

• **Principle of the K-means Clustering Algorithm**

K-means is an iterative clustering analysis algorithm [30]. The core idea is to partition a dataset of n objects into K clusters, such that the sum of the distances between each object and the center (or centroid) of its assigned cluster is minimized. The algorithm aims to ensure that objects within the same cluster are as close to each other as possible, while objects in different clusters are as separated as possible.

- **Initialization:** Select K data points as the initial cluster centers.
- **Assignment:** Assign each data point to the nearest cluster center.

For each data point in the dataset, compute its distance to each cluster center and assign it to the cluster center that is closest. This step typically uses Euclidean distance as the distance metric, calculated as follows:

$$\mathrm{dis}(x, c_i) = \sqrt{\sum_{j=1}^{d} (x_j - c_{ij})^2} \tag{8}$$

where $\mathrm{dis}(x, c_i)$ represents the Euclidean distance between the data point x and the i-th cluster center c_i. It is the target value calculated by the entire formula, which measures the distance between the two in a d-dimensional space; x represents a d-dimensional data point. Here, x_j is the value of the data point x in the j-th dimension, describing the characteristics of the data point in each dimension. c_i represents the i-th cluster center. c_{ij} is the value of the i-th cluster center in the j-th dimension, depicting the characteristic position of the cluster center in each dimension.

• **Update:** Recalculate the center of each cluster.

For each cluster, recalculate its center. The new cluster center is the mean of all data points within that cluster, computed as follows:

$$c_i = \frac{1}{|S_i|} \sum_{x \in S_i} x \tag{9}$$

where S_i represents the set of data points in the i-th cluster and $|S_i|$ denotes the number of data points in this set.

• **Stopping Conditions for Cluster Center Updates**

The clustering process terminates when one of the following conditions is met:

1) No significant change in cluster centers: The new cluster centers do not differ significantly from the old cluster centers, meaning the distance between them is less than a predefined threshold.
2) Maximum iterations reached: To prevent the algorithm from running indefinitely, a maximum number of iterations is set as a stopping criterion.

• **Principle of MTCMO Algorithm**

As illustrated in Figure 4, this study compares the performance and global optimality of four multi-objective optimization algorithms: NSGA-II, MOPSO, MOCell, and MTCMO.

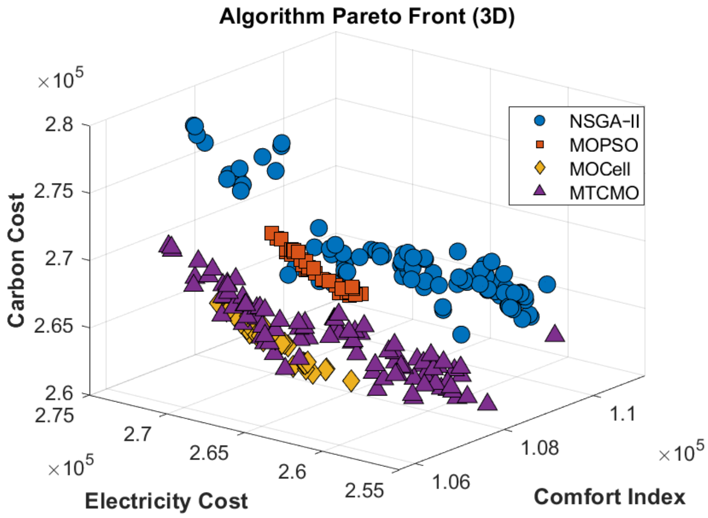

FIGURE 4. Algorithm comparison chart

The first three algorithms – NSGA-II (non-dominated sorting genetic algorithm II), MOPSO (multi-objective particle swarm optimization), and MOCell (multi-objective cellular evolutionary algorithm) – are widely recognized benchmark algorithms in the field of multi-objective optimization. They are selected for comparison due to their strong representativeness across different algorithmic paradigms: NSGA-II is based on evolutionary strategies, MOPSO employs swarm intelligence, and MOCell utilizes spatially structured population models. These methods have been extensively used and validated in energy management and scheduling problems, providing a solid baseline for performance benchmarking.

The MTCMO algorithm (multi-tasking co-evolutionary multi-objective optimization), proposed in this study, integrates multi-tasking evolutionary principles with co-evolution strategies to address the challenges of solution diversity and convergence in high-dimensional multi-objective scheduling problems. MTCMO simultaneously optimizes across multiple sub-populations while leveraging knowledge transfer among tasks, which enhances global search ability and reduces the likelihood of premature convergence to local optima.

As shown in the Pareto front plots, MTCMO outperforms the benchmark algorithms by offering a solution set characterized by both lower numerical values in electricity cost, carbon cost, and comfort deviation, as well as broader coverage across the objective space. This indicates superior performance in terms of both global optimality and distribution, making it particularly suitable for the complex trade-offs inherent in low-carbon, comfort-aware energy scheduling scenarios.

The ε-constraint-dominance method used in this paper is applied in two aspects:

1) It allows the temperature to fluctuate within the range of $[T_{\min} - \varepsilon_T, T_{\max} + \varepsilon_T]$;
2) It permits the switching frequency to briefly exceed $\Delta u_{\max}$ (with the violation amount $\leq \varepsilon_u$).

These two constraints ensure user comfort (temperature constraint) and equipment safety (switching constraint). Meanwhile, they expand the search space through controllable relaxation, thus preventing the scheduling scheme from falling into a local optimum.

3.3. **Optimization control constraints.** The temperature settings must ensure that the indoor room temperature remains within a reasonable range of user comfort for a

Table 1. Pseudocode for the MTCMO algorithm

Algorithm MTCMO
Input: Population Size NP, Maximum Iterations MaxIter
Initialization:
    P1 = Random Initialization(NP)
    P2 = Random Initialization(NP)
    Evaluate(P1)
    Evaluate(P2)
Main Loop:
    while Current Iteration < MaxIter:
        O1 = Generate Offspring(P1, NP/2)
        O2 = Generate Offspring(P2, NP/2)
        Evaluate(O1)
        Evaluate(O2)
        CombinedP1 = Combine(P1, O1)
        CombinedP2 = Combine(P2, O2)
        P1 = CDP Update(CombinedP1) #Constraint Domination Principle
        P2 = ε Update(CombinedP2) #ε-constraint Dominance Method
Output: Best Solution = Select Best from P1 and P2
 # Auxiliary Functions
Function Random Initialization(NP): Generate Random Individuals
Function Evaluate(Population): Compute Fitness
Function Generate Offspring(P, NP/2): Create New Individuals
Function Combine(Pop1, Pop2): Merge Populations
Function CDP Update(Population): Update using CDP Method
Function ε Update(Population): Update using ε Method
ε Represents the Constraint Relaxation Threshold for Controlling the Feasibility of the Solution

single air conditioner. The temperature constraints for the indoor room should be as follows:

$$T_{\min} \leq T^{\text{in}}(t) \leq T_{\max} \tag{10}$$

The constraints related to the switch status, timing, and number of air conditioners are as follows: Operating status: $k_z(t) = 1$ indicates working, and $k_z(t) = 0$ indicates standby; this model can be extended to Z heterogeneous air conditioning units on S time scheduling scale values.

$$\begin{cases} k_z(t) \in \{0, 1\}; \\ z = 1, 2, \ldots, Z; \ \ s = 1, 2, \ldots, S \end{cases} \tag{11}$$

3.4. **The criterion construction of AHP.** In this paper, a sequential approach is adopted, which first conducts multi-objective optimization and then uses AHP for comprehensive evaluation. This sequence is widely applied to problems such as power dispatch optimization and multi-objective energy management. The specific steps are as follows. First, a multi-objective optimization algorithm is employed to generate the Pareto front (the set of non-dominated solutions). Then, AHP is utilized to select the optimal solution or a weighted ranking scheme from it.

In this paper's design, under the premise of meeting the basic requirements of user comfort, the exploration focuses on reducing electricity cost and carbon emission cost.

The given priority order is comfort > carbon emission cost > electricity cost. We define comfort as (C1), carbon emission cost as (C2), and electricity cost as (C3). The comparison results are as follows: C1 is more important than C2, with a scale value of 5 (significantly important); C1 is more important than C3, with a scale value of 7 (strongly important); C2 is more important than C3, with a scale value of 3 (slightly important). Therefore, in the AHP, based on the above-mentioned scale values, the judgment matrix A is constructed as follows:

$$A = \begin{bmatrix} 1 & 5 & 7 \\ 1/5 & 1 & 3 \\ 1/7 & 1/3 & 1 \end{bmatrix} \tag{12}$$

1) By calculating the maximum eigenvalue $\lambda_{\max}$ and the corresponding eigenvector of matrix A, the weight vector is obtained after normalization.

$$w = \begin{bmatrix} 0.714 \\ 0.192 \\ 0.094 \end{bmatrix} \tag{13}$$

According to the calculation results, the weight allocation is as follows: comfort accounts for 71.4%, carbon emission cost accounts for 19.2%, and electricity cost accounts for 9.4%.

2) To verify the logical rationality of the judgment matrix, a consistency test is performed by calculating the consistency index (CI) and the random consistency ratio (CR).

First, the consistency index (CI) is calculated as

$$\lambda_{\max} = 3.094,\ CI = \frac{\lambda_{\max} - n}{n-1} = \frac{3.094 - 3}{3-1} = 0.047 \tag{14}$$

Then, the random consistency index (RI) is determined. When $n = 3$, $RI = 0.58$. Finally, the consistency ratio (CR) is computed as

$$CR = \frac{RI}{CI} = \frac{0.047}{0.58} = 0.081 < 0.1 \tag{15}$$

3) The judgment matrix passes the consistency test, verifying that the priority coefficients designed in this paper are correctly set.

4. **Case Study Analysis.** For the numerical selection of Z heterogeneous air conditioning units across S time scheduling intervals, we refer to the California Energy Demand Forecast, 2022-2035. Specifically, we base the number of units on the median participation scale (1,800-2,200 units) in California residential demand response (DR) programs [31]. Additionally, we adopt the standard 24-period division for day-ahead scheduling time to ensure consistency and comparability with existing research and practices [32]. Designing a region has $Z = 2{,}000$ air conditioning units and given that users have varying preferences for indoor temperatures, we design that the initial temperature settings of these air conditioning units follow a uniform distribution $U(25, 27)$; we adopt $S = 24$ period division for day-ahead scheduling time. Since the air conditioning units are located in different environmental spaces, their thermal equivalent parameters often exhibit uncertainty. Therefore, we assume that the thermal equivalent parameters of the air conditioners are randomly selected within a small range. The resulting air conditioning load parameters are shown in Table 2. As shown in Table 3, under the ideal indoor temperature settings for the air conditioners, the temperature settings of all air conditioning loads are increased by 1°C, 2°C, and 3°C, respectively. The resulting ideal indoor temperature curves for different temperature settings are illustrated in Figure 5.

TABLE 2. Air conditioning load parameter

	Thermal resistance R (°C/kW)	Heat capacity C (kWh/°C)	Refrigeration energy efficiency ratio N	Refrigeration power P (kW)
Upper limit	0.8	1.5	6	4
Lower limit	0.6	0.6	2.5	1

TABLE 3. User willingness under different temperature settings

	Air conditioning load curve	Willngness level 1	Willngness level 2	Willngness level 3
Increase temperature (°C)	0	1	2	3

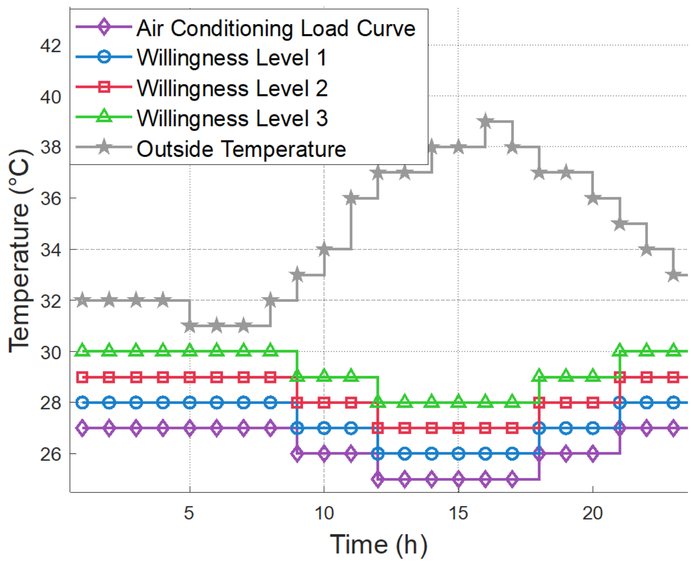

FIGURE 5. Ideal indoor air conditioning temperature under different setpoints

Figure 6 presents a comparison of the average carbon emission factors for the electricity grid in Jiangsu Province for the year 2022, along with real-time dynamic electricity carbon emission factors obtained from "the ecarbon+platform" developed by Tsinghua University, Hohai University, the Jiangsu Provincial Electric Power and Energy Efficiency Engineering Technology Center and State Grid Jiangsu Electric Power Company. This simulation comparison between the two average electricity carbon emission factors and dynamic electricity carbon emission factors assists in evaluating carbon emission costs for subsequent research. Additionally, it provides the 24-hour time-of-use electricity pricing applied in this study.

Figure 7 presents a comparative analysis of diurnal load profiles for an air conditioning cluster under dynamic carbon emission scenarios across four user willingness categories. The results reveal that baseline temperature settings (no adjustment) exhibit maximum hourly energy demand compared to modified scenarios, primarily due to extended operational durations required to maintain lower thermal comfort levels. Conversely, higher temperature setpoint adjustments demonstrate a consistent inverse relationship with daily energy consumption, showing progressively reduced power demand across willingness tiers. These findings collectively validate the temperature-dependent energy consumption

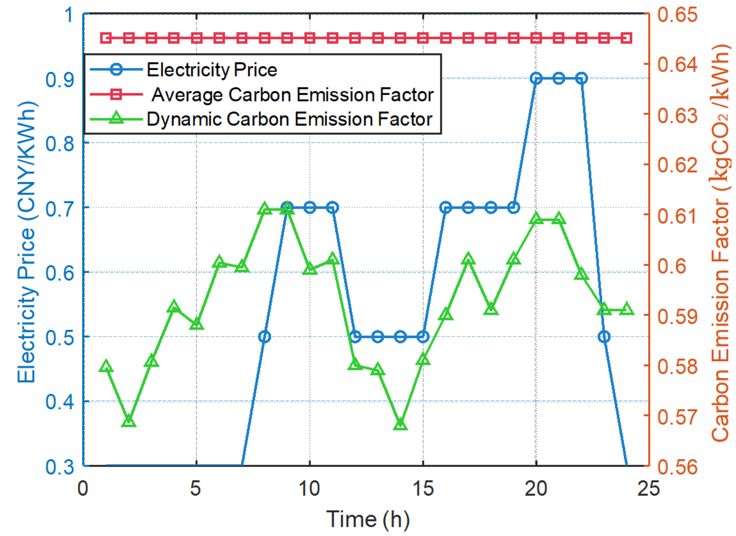

FIGURE 6. Two types of electricity carbon emission factors and time-of-use pricing chart

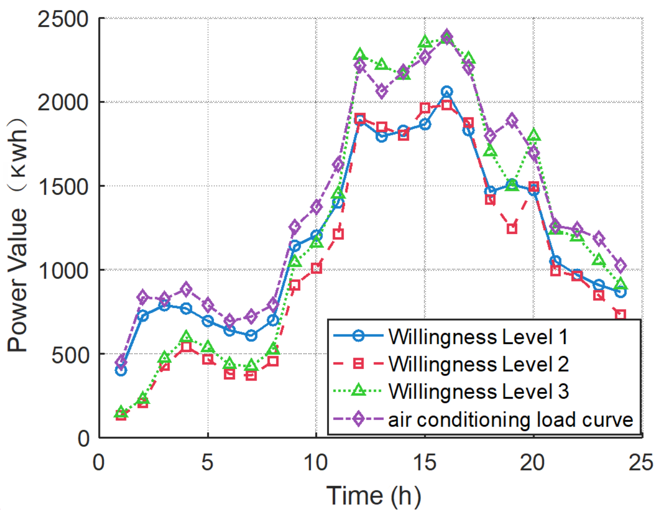

FIGURE 7. Daily load curves under different willingness levels

mechanisms in HVAC systems, establish empirical consistency with real-world operational data patterns and confirm the methodological relevance of incorporating user preference heterogeneity into carbon-aware energy optimization.

Figure 8 presents the 24-hour indoor temperature profiles achieved by the 1000th air conditioner under four distinct user willingness categories following cooling operations. The results demonstrate that across all investigated preference levels, the optimization framework successfully maintains predefined thermal comfort boundaries. This fundamental outcome validates the research's dual objectives: ensuring occupant thermal comfort as a primary constraint while achieving cost-effective carbon and electricity consumption optimization. By fulfilling both requirements simultaneously, the study establishes empirical evidence of the proposed method's capability to balance human comfort priorities with sustainable energy management in building systems.

Figure 9 illustrates the user comfort, electricity cost and carbon emission cost for 2000 air conditioning units based on user willingness level 1 under both average and dynamic

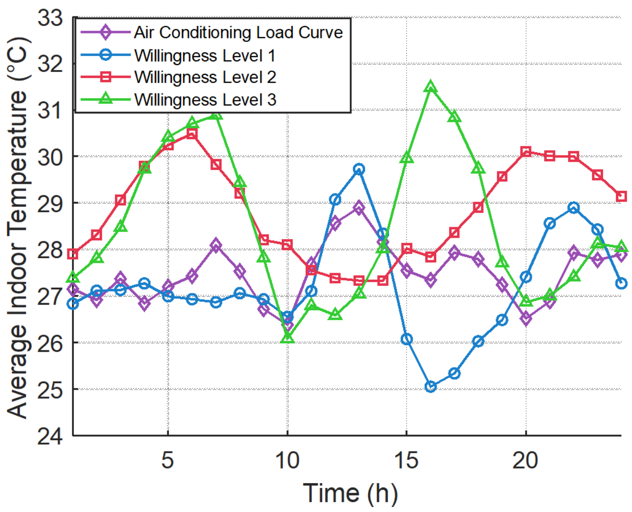

FIGURE 8. Indoor temperature adjustment curves under different willingness levels

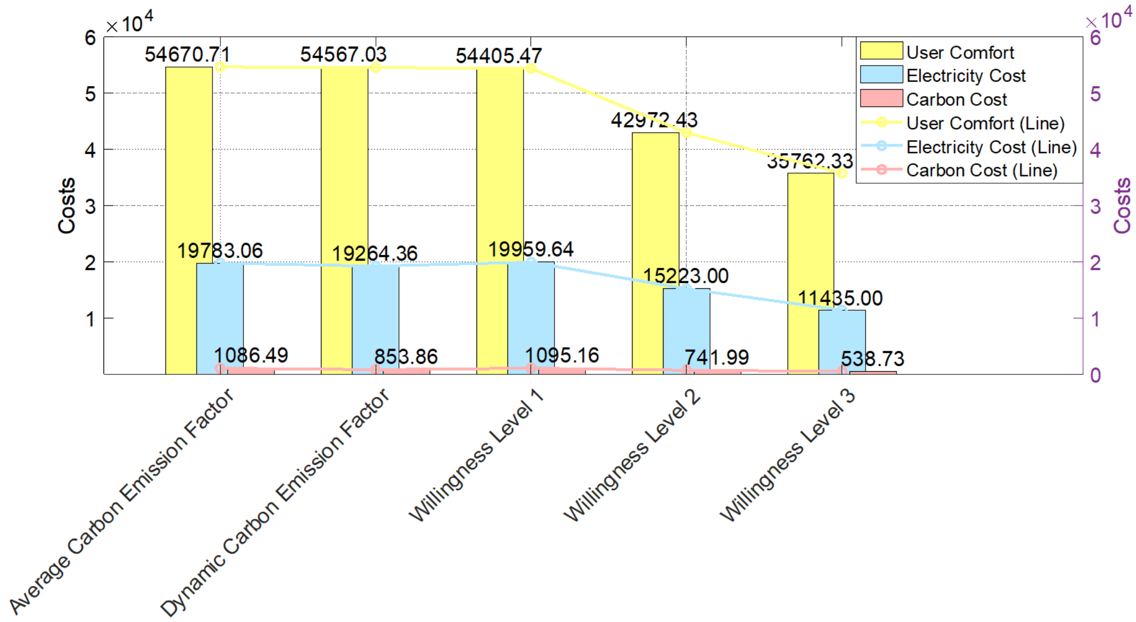

FIGURE 9. Tri-objective results under two electricity carbon emission factors

electricity carbon emission factors. It also shows these factors under user willingness levels 1, 2, and 3 with dynamic electricity carbon emission factors. The analysis reveals that under comparable thermal comfort conditions (willingness level 1), implementing dynamic carbon emission pricing mechanisms achieves reductions of 518.7 RMB and 232.61 RMB in electricity and carbon costs, respectively. This quantifiable outcome demonstrates pronounced cost-savings potential through integrated carbon-aware energy optimization, confirming the economic viability of dynamic emission factor incorporation in building energy management systems. Regarding the user comfort, electricity cost, and carbon emission cost under dynamic electricity carbon emission factors at willingness levels 1, 2, and 3, there is considerable variation in comfort performance metrics across different user willingness levels. As shown in Figure 8, varying user preferences for indoor temperature result in different comfort requirements, which aligns with the observed variations in comfort performance metrics. Meanwhile, under dynamic electricity carbon emission factors, both electricity and carbon emission costs are significantly reduced.

In this paper, air conditioners with different parameters were classified and controlled in groups based on aggregation classification, and the load potential of air conditioners was further evaluated. When the clustering method was not adopted for the four parameters of air conditioners, namely thermal resistance, heat capacity, refrigeration energy efficiency ratio and refrigeration rated power, 2000 air conditioners each had their own switching control strategy. This makes the optimization process very time-consuming. If we adopt the clustering method of the basic parameters of air conditioners, the air conditioners clustered into the same cluster group will adopt a unified switching strategy which will greatly improve the solving efficiency. K-means clustering method and elbow method were used to determine the optimal number of clusters into 9 categories. Figure 10 depicts the process of selecting fundamental physical quantities for clustering and determining the optimal number of clusters in this study.

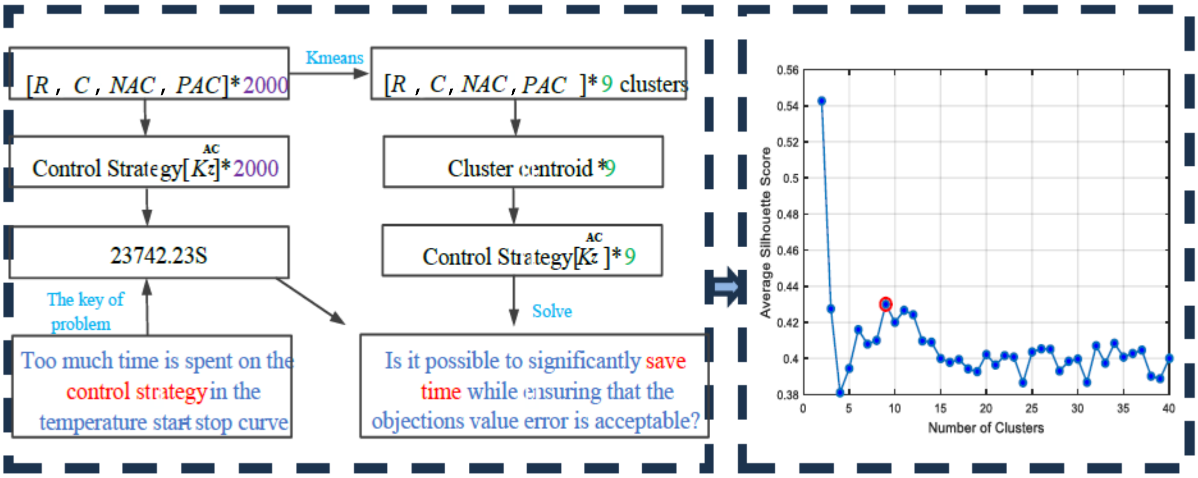

FIGURE 10. Framework of cluster writing

Table 4 illustrates the comparison of optimization objectives and computation times before and after clustering. It can be seen that the time saved after clustering is equivalent to 97.58% of that before clustering which greatly saves time; at the same time, the comfort index has a fluctuation of 7.92% which means that the air conditioner parameters of the cluster center are used as input to obtain a unified switching strategy in the cluster where the 2000 air conditioners are located ignoring the refined switching strategy control for each air conditioner resulting in the sacrifice of some user comfort; the electricity cost and carbon emission cost have fluctuations of 23.23% and 27.53%, respectively.

TABLE 4. Computation time and objective function values for unclustered and clustered approaches

	Time (s)	Comfort index	Electricity cost (CNY)	Carbon cost (CNY)
Unclustered numeric	23742.23	54567.03	19264.36	853.86
Clustered numeric	573.46	58890.63	23738.84	1088.93
Change numeric	23168.77	4323.6	4474.48	309.49
Numeric percentage	−97.58%	+7.92%	+23.23%	+27.53%

In the large-scale air conditioner cluster number and algorithm input variables, the work of this paper can provide a reference for the rapid evaluation of the potential of massive air conditioner regulation.

5. **Conclusions.** A multi-objective optimization framework is formulated for coordinated control of large-scale air conditioning systems under dynamic carbon pricing scenarios. The framework integrates three critical objectives – occupant thermal comfort, electricity cost minimization, and carbon emission reduction – through parametric modeling of individual air-conditioner units. By incorporating four representative temperature setpoints corresponding to different user willingness levels, the model quantifies the trade-off between comfort preferences and energy costs.

Optimal control parameters are derived using a constrained optimization algorithm that balances system-level efficiency with distributed device-specific characteristics. A key innovation lies in the proposed clustering-based computational approach which aggregates similar device operational patterns into homogeneous groups. This methodological advancement enables significant computational efficiency gains by reducing the problem complexity from individual device control to group-level strategy formulation. The resultant unified control scheme demonstrates both technical feasibility and practical applicability in achieving carbon-efficient energy management for building-scale HVAC systems. Comparative case studies indicate

1) The strategy ensures user comfort under different user responsiveness levels, demonstrating good adaptability.
2) The three-objective competitive equilibrium problem based on dynamic carbon emission factors effectively reduces costs and provides more accurate and fair outcomes.
3) The method of clustering similar air conditioner parameters to derive a unified control strategy can be used as a rapid assessment method for the potential of reducing electricity and carbon costs in large-scale air conditioning systems within an acceptable error range.

Future research should focus on

1) Integration with renewable generation forecasting: developing coupled models that synchronize HVAC control with solar/wind power prediction to enhance grid-responsive capability;
2) Cross-building coordination: Extending the clustering approach to heterogeneous building clusters with varying thermal characteristics and occupancy patterns;
3) Adaptive willingness modeling: Creating dynamic user willingness models that evolve based on historical behavior and real-time environmental stimuli.

Acknowledgment. This work is supported by Guangdong Provincial Key Laboratory of Intelligent Measurement and Advanced Metering of Power Grid (GPKLIMAMPG-2023-KF-01). The authors also gratefully acknowledge the helpful comments and suggestions of the reviewers, which have improved the presentation.

REFERENCES

[1] An electric power and energy balance optimization model based on wind power capacity credit, *2018 IEEE PES Asia-Pacific Power and Energy Engineering Conference (APPEEC)*, Kota Kinabalu, Malaysia, pp.172-177, 2018.

[2] X. Zhang, Y. Wei and X. Liu, The impact of carbon pricing on electricity prices: A case study of China, *Energy Policy*, vol.135, 111006, 2019.

[3] I. E. Parra-Olea, J. M. Gómez-García and F. J. Gómez-Aguilar, The critical role of demand response in future power systems: A multi-disciplinary perspective, electricity generation, *Transmission and Distribution*, vol.158, no.6, 2022.

[4] L. Zhang, Y. Li and H. Chen, Carbon-aware demand response and renewable integration in power systems, *IEEE Transactions on Power Systems*, vol.37, no.4, pp.3122-3133, 2022.
[5] S. M. A. Alavi, A. H. M. Shafie-khah and S. A. Hosseini, A data-driven approach for demand response of air conditioning systems using LSTM neural networks, *IEEE Transactions on Smart Grid*, vol.9, no.3, pp.1672-1683, 2019.
[6] China Association of Building Energy Efficiency, *China Building Energy Consumption and Carbon Emissions Research Report 2023*, Beijing, 2023.
[7] N. G. Paterakis, A. Taşcıkaraoğlu, O. Erdinç, A. G. Bakirtzis and J. P. S. Catalão, Assessment of demand-response-driven load pattern elasticity using a combined approach for smart households, *IEEE Transactions on Industrial Informatics*, vol.12, no.4, pp.1529-1539, 2016.
[8] G. Ruan, H. Zhong, J. Wang, Q. Xia and C. Kang, Neural-network-based Lagrange multiplier selection for distributed demand response in the smart grid, *Applied Energy*, vol.264, 114636, 2020.
[9] Y. Chen, L. Zhang and H. Li, Demand response of air conditioning systems via reinforcement learning for grid frequency regulation, *Energy and Buildings*, vol.215, no.3, 108680, 2020.
[10] L. H. Tsoukalas and R. Gao, From smart grids to an energy internet: Assumptions, architectures and requirements, *2008 3rd International Conference on Electric Utility Deregulation and Restructuring and Power Technologies*, Nanjing, China, pp.94-98, 2008.
[11] F. Langner, M. Frahm and W. Wang, Hierarchical-stochastic model predictive control for a grid-interactive multi-zone residential building with distributed energy resources, *Journal of Building Engineering*, vol.89, 109401, https://doi.org/10.1016/j.jobe.2024.109401, 2024.
[12] M. Li, Y. Zou and J. Chen, Stochastic model predictive control for building energy systems with weather uncertainty, *Energy and Buildings*, vol.178, no.3, pp.188-199, 2019.
[13] Y. G. Song, M. C. Xia, Q. F. Chen and F. J. Chen, A data-model fusion dispatch strategy for the building energy flexibility based on the digital twin, *Applied Energy*, vol.332, 120496, https://doi.org/10.1016/j.apenergy.2022.120496, 2023.
[14] H. Li, Y. Chen and L. Zhang, Coordinated control of HVAC fans and battery storage for frequency regulation in smart grids, *IEEE Transactions on Industrial Informatics*, vol.16, no.5, pp.3240-3250, 2020.
[15] H. AbdelRaouf et al., Demand response in smart grids: Challenges, solutions, and security implications, *2024 2nd International Conference on Artificial Intelligence, Blockchain, and Internet of Things (AIBThings)*, Mt Pleasant, MI, USA, pp.1-6, 2024.
[16] Z. Y. Feng and J. Zhang, Energy consumption prediction strategy for electric vehicle based on LSTM-transformer framework, *Energy*, vol.302, 131780, https://doi.org/10.1016/j.energy.2024.131780, 2024.
[17] J. Zhou, Y. Wu and Y. Wang, Clustering-based temperature control for air conditioning load management, *IEEE Transactions on Industrial Informatics*, vol.14, no.5, pp.2069-2078, 2018.
[18] P. H. Shaikh, N. B. A. Rahim, T. N. Yang and P. R. Singh, Hourly temperature-power co-optimization for efficient HVAC load scheduling, *Energy Reports*, vol.5, no.5, pp.1247-1258, 2019.
[19] L. Li, Multi-source information data integration method founded on K-medoids clustering algorithm, *International Journal of Innovative Computing, Information and Control*, vol.19, no.6, pp.1877-1890, 2023.
[20] K. Ni, A clustering algorithm combining fuzzy C-Means and artificial bee colony algorithm, *International Journal of Innovative Computing, Information and Control*, vol.20, no.1, pp.297-311, 2024.
[21] J. X. Wang, H. W. Zhong and Z. M. Ma, Review and prospect of integrated demand response in the multi-energy system, *Applied Energy*, vol.2, no.4, pp.772-782, 2017.
[22] A. Abdulla and G. Baryannis, A hybrid multi-criteria decision-making and machine learning approach for explainable supplier selection, *Supply Chain Analytics*, vol.7, 100074, https://doi.org/10.1016/j.sca.2024.100074, 2024.
[23] Y. Sun, M. Zhou, Q. Zhang and T. Liu, Peak shaving control of residential air conditioners for demand response aggregation using switch control, *Energy Reports*, vol.6, no.4, pp.1115-1122, 2020.
[24] Y. Wu, Y. Zhang and X. He, Optimal switch control of air conditioners for peak load reduction considering customer comfort, *IEEE Transactions on Smart Grid*, vol.11, no.1, pp.157-168, 2020.
[25] S. Liu, H. Sun and Z. Wang, Demand response for peak shaving using on/off control of air conditioners in a multi-zone building, *Applied Energy*, vol.195, no.3, pp.1041-1052, 2017.
[26] N. Zhang and Z. Lv, A two-stage process bat algorithm for solving the steelmaking and continuous casting scheduling problem with energy constraints, *International Journal of Innovative Computing, Information and Control*, vol.19, no.4, pp.1117-1138, 2023.

[27] L. Ji, H. Zheng and J. Zhang, Dynamic carbon emission factor perception method for power users based on carbon emission flow theory, *Journal of Cleaner Production*, vol.212, no.2, pp.1256-1266, 2019.
[28] H. Chen, J. Wang, Y. Song and Z. Zhang, Carbon flow modeling and analysis for power systems with low carbon operation, *Energy Procedia*, vol.158, no.5, pp.3779-3784, 2019.
[29] Y. He, X. Wu, H. Yang and Q. Xia, A carbon emission flow-based approach for calculating carbon emission costs in the power system, *Applied Energy*, vol.240, no.6, pp.505-514, 2019.
[30] X. Wang, Y. Li and J. Zhang, Deep clustering for load pattern recognition in smart grids, *IEEE Transactions on Smart Grid*, vol.13, no.5, pp.4023-4034, 2022.
[31] *California Energy Demand Forecast, 2022-2035*, 2022 Integrated Energy Policy Report, California Energy Commission, 2022.
[32] *IEEE Standard for Smart Energy Profile Application Protocol in IEEE Std 2030.5-2023 (Revision of IEEE Std 2030.5-2018/Incorporates IEEE Std 2030.5-2023/Cor1-2024)*, pp.1-398, 2024.

Author Biography

Ji Wang received bachelor's degree in Electrical Engineering from Guizhou University, China, in 2009. In 2012, she received master's degree in Electrical Engineering from the same university. She is currently a Senior Engineer with CSG Electric Power Research Institute, China and Guangdong Provincial Key Laboratory of Intelligent Measurement and Advanced Metering of Power Grid, China. Her research interests include intelligent measurement, vehicle network interaction, and charging facility detection.

Jianlin Tang received bachelor's degree in Electrical Engineering from South China University of Technology, China, in 2017. In 2020, he received master's degree in Electrical Engineering from the same university. He is currently an Engineer with CSG Electric Power Research Institute, China and Guangdong Provincial Key Laboratory of Intelligent Measurement and Advanced Metering of Power Grid, China. His research interest includes measurement electricity and its carbon.

Fan Zhang received bachelor's degree in Electrical Engineering from Wuhan University, China, in 2018. In 2021, he received master's degree in Electrical Engineering from the same university. He is currently an Engineer with CSG Electric Power Research Institute, China and Guangdong Provincial Key Laboratory of Intelligent Measurement and Advanced Metering of Power Grid, China. His research interests include electricity measurement and its terminal equipment, interaction between electric vehicles and power grid.

Dawei Ren received bachelor's degree in Energy and Power Engineering from Liaoning Technical University, China, in 2021. He is a master student of Foshan Graduate School of Innovation, Northeastern University, China now. His research interests include electric power carbon emission monitoring and measurement technology and user demand response modeling in the electrocarbon coupling market environment.

Zhengxun Guo received bachelor's degree in Electrical Engineering from Kunming University of Science and Technology, China, in 2020. In 2023, he received master's degree in Electrical Engineering from the same university. He is a Ph.D. student at Foshan Graduate School of Innovation, Northeastern University, China now. His research interests focus on carbon emission reduction of distribution network, dispatch and control of distribution network, development and application of intelligence algorithms, and system optimization of renewable energy.